Published in final edited form as:
FASEB J. 2008 April ; 22(4): 1246–1257.

Role of the Acidic N′-Region of Cardiac Troponin I In Regulating Myocardial Function*

Sakthivel Sadayappan[‡], **Natosha Finley**[§], **Jack W Howarth**[§], **Hanna Osinska**[‡], **Raisa Klevitsky**[‡], **John N Lorenz**[¶], **Paul R Rosevear**[§], and **Jeffrey Robbins**[‡,1]

‡*Division of Molecular Cardiovascular Biology, Department of Pediatrics, Cincinnati Children's Hospital Medical Center, 3333 Burnet Ave., Cincinnati, OH 45229*

§*Molecular Genetics, Biochemistry and Microbiology, 231 Bethesda Ave, ML 0542, University of Cincinnati, Cincinnati, OH 45267*

¶*Molecular and Cellular Physiology, Department of Medicine, 231 Bethesda Ave, ML 0542, University of Cincinnati, Cincinnati, OH 45267*

Abstract

Cardiac troponin I (cTnI) phosphorylation helps regulate myocardial contractility and relaxation during β-adrenergic stimulation. cTnI differs from the skeletal isoform in that it has a cardiac specific N′-extension of 32 residues (N′-extension). The role of the acidic-N′-region in modulating cardiac contractility has not been fully defined. To test the hypothesis that the acidic-N′-region of cTnI helps regulate myocardial function, we generated cardiac-specific transgenic mice in which residues 2–11 ($cTnI^{\Delta 2-11}$) were deleted. The hearts displayed significantly decreased contraction and relaxation under basal and β-adrenergic stress compared to non-transgenic hearts, with a reduction in maximal Ca^{2+} dependent force and maximal Ca^{2+}-activated Mg^{2+}-ATPase activity. However, Ca^{2+} sensitivity of force development and cTnI-$Ser^{23/24}$ phosphorylation were not affected. NMR amide proton/nitrogen chemical shift analysis shows that phosphorylation at $Ser^{23/24}$ in cTnI and $cTnI^{\Delta 2-11}$ decrease interactions with the N-lobe of cardiac troponin C. We hypothesized that phosphorylation at $Ser^{23/24}$ induces a large conformational change positioning the conserved acidic-N-region to compete with actin for the inhibitory region of cTnI. Consistent with this hypothesis, deletion of the conserved acidic-N′-region results in a decrease in myocardial contractility in the $cTnI^{\Delta 2-11}$ mice demonstrating the importance of acidic-N′-region in regulating myocardial contractility and mediating the heart's response to β-AR stimulation.

Keywords

muscle; transgenic mouse model; contractility; heart

INTRODUCTION

β-adrenergic (β-AR) signaling plays a fundamental role in regulating cardiac performance (1). Physiological effects include increases in contractile force, heart rate and the rate of relaxation. The use of β-AR agonists and β-AR blockers to treat acute ventricular failure or chronic failure, respectively, likely represent a delicate balance of different cardioprotective mechanisms. During β-AR stimulation, multiple proteins in the sarcolemma, sarcoplasmic reticulum and myofilament are phosphorylated at multiple sites. One of the sarcomeric

1Correspondence to: Division of Molecular Cardiovascular Biology, Cincinnati Children's Hospital Medical Center, MLC 7020, 3333 Burnet Ave, Cincinnati, OH 45229-3039 Tel: (513) 636-8098; Fax: (513) 636-5958. E-mail: jeff.robbins@cchmc.org.

proteins, cTnI, is a key regulatory protein of the thin filament. There are three closely related troponin I (TnI) genes, each of which is selectively expressed in either the cardiac, fast skeletal or slow skeletal muscle fibers. The embryonic heart expresses mostly slow skeletal muscle TnI but expression gradually decreases during prenatal heart development as cTnI increases and becomes the only TnI isoform in the adult heart (2–4). Cardiac TnI interacts with the major proteins present in the sarcomeric thin filament, including actin, cTnC, α-tropomyosin (α-TM) and troponin T (cTnT). These interactions underlie its central role as a molecular switch, regulating muscle contraction in response to changes in intracellular Ca^{2+} concentrations.

Cardiac TnI differs from the slow skeletal isoform of TnI in that it contains a 32 amino acid (31 in the human) N′-extension. cTnI's N′-extension is composed of three regions; an acidic-N′-region containing a single turn of helix, an extended rigid polyproline helix, and a C′-helix containing the bisphosphorylation motif. The β-AR signaling pathway controls phosphorylation of the two serine residues ($Ser^{23/24}$) in the N′-extension by cAMP-dependent protein kinase (PKA) (5) and protein kinase D (PKD) (6). Phosphorylation of $Ser^{23/24}$ results in a reduction in myofilament Ca^{2+} sensitivity (1) and an increase in cross-bridge cycling rate (7) by reducing the Ca^{2+} binding affinity of cTnC and allowing fine tuning of contractile function (8). This mechanism plays an important role in the functional adaptation of cardiac muscle to physiological or pathological stress.

Molecular modeling data have enabled predictions to be made and tested for cTnI's functional domains. In the non-phosphorylated state, the N′-extension interacts with cTnC's inactive Ca^{2+} binding site I and helix A, largely through a series of weak electrostatic and hydrophobic interactions such that the acidic-N′-region is does not strongly contact cTnC (9–11). However, an important unanswered question is the role of the conserved acidic-N′-region of cTnI in modulating cardiac function. Based on the available biochemical and physiological data, we hypothesized that modulation through phosphorylation might be partially mediated by electrostatic interactions between cTnI's acidic-N′-region and available basic regions in cTnI, altering cross-bridge kinetics. Thus, the role of phosphorylation would be to stabilize a conformation able to facilitate these ionic interactions. Phosphorylation-induced loss of interaction with the N′-lobe of cTnC probably induces a hinge movement of the rigid PPII helix, positioning cTnI's acidic-N′-region for electrostatic interaction with the conserved basic region of cTnI. The PPII helix is well suited for such conformational movement due to its restricted conformational rigidity, solvent exposure, and ability to present a hydrophobic surface as well as hydrogen bonding sites. Consistent with this hypothesis, NMR and modeling studies showed that bisphosphorylation of cTnI at $Ser^{23/24}$ resulted in extension of its position on the N′-lobe of cTnC and interaction with the basic inhibitory region of cTnI (10).

To determine the role of the acidic-N′-region of cTnI on cardiac contractile function, we generated transgenic (TG) mice with cardiomyocyte-specific postnatal overexpression of a truncated cTnI that lacks the acidic-N′-region ($cTnI^{\Delta 2-11}$). $cTnI^{\Delta 2-11}$ cardiac myofibrils showed reductions in both maximal Mg^{2+}-ATPase activity and absolute force, but no changes in Ca^{2+} affinity. $cTnI^{\Delta 2-11}$ hearts had significantly reduced rates of contraction and relaxation under baseline and β-agonist treatment. These findings indicate that the acidic-N′-region of cTnI plays an important role in regulating cardiac function in non-stimulated hearts as well as during β-AR stimulation.

MATERIAL AND METHODS

Generation of TG mice

To investigate the role of the acidic-N′-region of cTnI on cardiac contractile function, we generated a cDNA that encodes mouse cTnI with a deletion of residues 2–11 (ADESSDAAGE). The full-length mouse wild-type (WT) cDNA cTnI was obtained by reverse

transcription-PCR using total RNA isolated from mouse cardiac ventricles. The cDNA containing $cTnI^{WT}$ fragments were initially subcloned into pBluescript and sequenced as described earlier (14). The 10 amino acids of the acidic-N′-region (Fig. 1*A*) were deleted by standard PCR-based methods ($cTnI^{\Delta 2-11}$). The $cTnI^{\Delta 2-11}$ cDNA was subcloned into a site immediately downstream of the mouse cardiac α-myosin heavy chain promoter (α-MyHC) and the sequence verified by DNA sequencing. The TG cassette was then released from the vector backbone using NotI digestion, followed by gel purification. Multiple lines of FVB/N TG mice were generated using the purified NotI-digested DNAs. Founder mice were identified by PCR using tail clip DNA as template. Transgene copy number was determined by Southern blot analysis using an α-MyHC promoter probe. The founders were bred to non-transgenic (NTG) mice and lines showing Mendelian patterns of transmission selected for further analysis. Five or six mice per experiment, 12–15 weeks old of mixed gender were used for our studies after pilot experiments showed no gender differences. All TG mouse lines were viable and fertile. The mice had a normal lifespan and no gross cardiovascular pathology presented. All protocols complied with the *Guide for the Use and Care of Laboratory Animals* published by the National Institutes of Health.

Molecular and protein analyses

Transcript levels were determined by RNA dot blot analysis with γ-^{32}P-labeled cTnI and human growth hormone as well as probes for the cardiac hypertrophic markers atrial natriuretic factor and β-MyHC (12). Myofibrillar proteins were isolated from NTG and $cTnI^{\Delta 2-11}$ mouse hearts using F60 buffer as previously described (8) and assayed for protein concentrations using the Bradford method (Bio-Rad, Hercules, CA, USA). The percentage of cTnI replacement was determined via SDS-PAGE (4–15% gradient Tris-HCl Ready Gel; Bio-Rad, Hercules, CA, USA) and Western blots using polyclonal antibodies against cTnI (Cell Signaling Technology, Danvers, MA, USA). Two-dimensional gel electrophoresis was carried out as described (8). Antibodies used for Western blot analysis are as follows: phospho-specific cTnI-$Ser^{23/24}$ (Cell Signaling Technology, Danvers, MA, USA), total phospholamban (PLN) (Upstate, Lake Placid, NY), phosphorylated PLN-Ser^{16} (Upstate, Lake Placid, NY, USA), phosphorylated PLN-Thr^{17} (Cyclacel, Dundee, UK), calsequestrin (Research Diagnostics, Flanders, NJ), cardiac myosin binding protein-C (cMyBP-C) C0–C1 domain (12), phospho-specific cMyBP-C^{Ser282} (generous gift of Lucie Carrier (13)), cardiac troponin T (Sigma, St. Louis, MO, USA) and cardiac α-tropomyosin (Chemicon, Temecula, CA, USA).

Histopathology and immunohistochemistry analyses

The heart weight (HW) and the ratio of heart weight:body weight (HW/BW) were measured to determine if cardiac hypertrophy had occurred. Gross examination and histopathological analysis were carried out as described (8). The paraffin-embedded longitudinal sections of whole mouse hearts stained with hematoxylin-eosin or Masson's trichrome were examined for overall morphology, presence of necrosis, fibrosis, myocyte disarray and calcification using an Olympus B-60 microscope and SPOT software (Diagnostic Instruments, Sterling Heights, MI, USA). Localization and integration of $cTnI^{\Delta 2-11}$ into the sarcomere was determined by confocal microscopy (12). Five-μm cryostat sections were probed with cTnI antibodies (Cell Signaling Technology, Danvers, MA, USA) followed by incubation with Alexa-488 conjugated secondary antibody (Invitrogen, Carlsbad, CA, USA).

Cardiac function and β-AR responsiveness

For two-dimensional M-mode echocardiography, mice with the implanted osmotic pumps were anesthetized with 2% isoflurane. Hearts were visualized with a Hewlett Packard Sonos 5500 instrument and a 15 MHz transducer (12). Measurements were taken three times per mouse from different areas and then averaged for left ventricular (LV) diastolic and systolic

dimensions and septal and posterior wall thickness, from which fractional shortening (FS) and LV mass was derived. Invasive hemodynamic studies was performed in the intact animals as previously described (14). Data were analyzed using a PowerLab system (ADInstruments, Colorado Springs, CO, USA).

Chronic isoproterenol (ISO) infusion

To determine the stress tolerance of $cTnI^{\Delta 2-11}$ hearts, NTG and $cTnI^{\Delta 2-11}$ animals underwent two weeks of continuous infusion of the β-agonist ISO (Sigma, St. Louis, MO). Alzet miniosmotic pumps (Durect Corporation, Cupertino, CA, USA) containing either ISO (60 mg/kg/day) in 0.02% ascorbic acid (Sigma) or vehicle only (sham) were surgically implanted between the scapulae in 12-week-old NTG and $cTnI^{\Delta 2-11}$ mice for 14 days as described (15). Cardiac function was measured by M-mode echocardiography before, 7, and 14 days after implantation.

In vitro PKA phosphorylation and Ca^{2+}-activated Mg^{2+}-ATPase assays

To phosphorylate myofibrillar proteins, total myofibrils were incubated with the catalytic subunit of PKA as described earlier (8). Ca^{2+}-activated Mg^{2+}-ATPase activity was measured by titrating $Ca^{2+\Delta}$sensitivity of the NTG and $cTnI^{\Delta 2-11}$ mouse hearts and measuring P_i release (8). Data were analyzed by fitting the data obtained for each individual and then averaging the derived Hill parameters as described (8).

In Situ fiber kinetics

Procedures for mechanical analysis of murine papillary fibers have been described (16,17). In brief, mice were injected with heparin (500 IU/kg intraperitonally) 5 min before being killed. To prepare skinned fibers, the heart was removed and placed in relaxing solution (5.37 mM ATP, 30 mM phosphocreatine, 5.0 mM EGTA, 20 mM BES, 7.33 mM $MgCl_2$, 0.12 mM $CaCl_2$, 10 mM DTE, 10μg/mL leupeptin, and 32 mM potassium methansulfonate, pH 7.0) at 4 °C. The solution also contained 30 mM 2,3-butanedione monoxime designed to protect myocardial tissue from mechanical injury. Muscle fibers of approximately 0.5-mm diameter and 2–3-mm length were isolated from left ventricular papillary muscles. The fiber strips were skinned by incubation in 5.5 mM ATP, 5.0 mM EGTA, 20 mM BES, 6.13 mM $MgCl_2$, 0.11 mM $CaCl_2$, 10 mM DTE, 10 μg/mL leupeptin, 121.8 mM potassium methansulfonate, pH 7.0, and 50% glycerol with 0.5% (wt/vol) Triton X-100 for 12 h at 4 °C. The fiber strips were then transferred to fresh solution without Triton X-100, and stored at −20 °C until used. Dissected fibers were mounted isometrically between a force transducer and a length-step generator in relaxing solution (Scientific Instruments, Heidelberg, Germany). Sarcomere length (determined by laser diffraction analysis) at resting tension was always 2.0–2.1 μm. We determined that the cross-sectional area at the base of the muscle was between 0.05 to 0.1 mm^2. Contraction solution had the same composition as the relaxing solution, except that EGTA was substituted with 5 mM [Ca^{2+}]EGTA. Initial maximum isometric force was measured in activating solution (*p*Ca 5.0). Force was determined while the fibers were bathed in sequentially increasing Ca^{2+} concentrations ranging from *p*Ca 8 to 5.0 *p*Ca values and recorded on a chart recorder. Strip tension (mN/mm^2) was calculated by dividing force by fiber cross-sectional area, calculated from widths measured at the major axis. To examine the effects of PKA phosphorylation on the *p*Ca-force relationship *in vitro*, skinned fibers were treated with PKA (Novagen, San Diego, CA, USA). After measurements of the pCa-force relationship (before PKA treated), the fiber was incubated in relaxing solution (*p*Ca 8.0) plus 0.5 μM PKA for 10 min. The fibers were relaxed for 15 min, and the *p*Ca-force relationship was measured after PKA treatment.

NMR spectroscopy and data processing

The cTnI^{WT} and cTnI$^{\Delta 2-11}$ cDNAs were subcloned into the pET23^{a+} expression vector (Novagen, San Diego, CA, USA). [^{15}N,^{2}H]cTnC, cTnI^{WT} and cTnI$^{\Delta 2-11}$ proteins were expressed in bacteria, purified and complex formation was carried out as described (23,24). NMR experiments were performed at 40 °C on Varian 600- or 800-MHz Inova spectrometers (25) and spectral widths in the t^1 and t^2 dimensions were 3.3 and 12 kHz, respectively. Composite amide chemical shift differences were determined from the square root of the weighted sum of the squares of proton and nitrogen chemical shift differences. ^{15}N chemical shift differences were weighted by a factor of one-seventh to scale their contributions to a magnitude similar to ^{1}H chemical shift differences and the data processed as described (24). Spectra were processed with Felix 2000 and analyzed with Sparky (T. D. Goddard and D. G. Kneller, Sparky3, University of California, San Francisco, CA, USA) software packages.

Statistical analysis

All values are expressed as means ± S.E. The statistical significance of differences between two groups and multiple groups was determined by Student's *t* test and two-way ANOVA (SigmaStat 3.1, Systat Software, San Jose, CA, USA), respectively. For all tests, $P<0.05$ was considered significant. The Hill coefficient was calculated using Origin 7.5 NLSF tool (OriginLab Corporation, Northampton, MA, USA) as described (8). The theoretical molecular weight and isoelectric point of cTnI were calculated at http://prometheus.brc.mcw.edu/promost/.

RESULTS

Cardiac specific expression of the cTnI$^{\Delta 2-11}$ transgene

To investigate the functional effects of cTnI's acidic N′-region (Fig. 1*A*) in intact mouse hearts we generated TG mice in which this region was deleted (cTnI$^{\Delta 2-11}$). The cDNA was linked to the mouse α-MyHC promoter to drive cardiac specific expression and used to generate multiple TG mouse lines. Nineteen TG lines were obtained with varying copy numbers as analyzed by Southern blot analysis. For all of the lines, normal Mendelian ratios were observed, indicating that expression did not result in any detectable embryonic lethality. The amount of TG transcript being expressed was determined for each line and three lines (lines 93, 81 and 78) were selected in which cTnI$^{\Delta 2-11}$ expression was roughly equivalent to a TG line that expresses high levels of normal cTnI (cTnI^{WT}) (Fig. 1*B*), which served as a control to rule out any phenotype that might occur merely as a result of high TG expression levels of cTnI. (18). Lines 93, 81 and 78 showed 5.5-, 4.0- and 2.8-fold increases over NTG controls, respectively (Fig. 1*C*). The sarcomere has the capacity to maintain protein stoichiometry even when the transcript levels are increased via TG manipulation. Thus the degree of replacement is a function of the level of overexpression (8). The degree of cTnI$^{\Delta 2-11}$ protein replacement was confirmed by SDS-PAGE (Fig. 2*A*) as well as by Western blots using cTnI-specific antibodies that recognize both the endogenous cTnI and TG cTnI$^{\Delta 2-11}$ proteins (Fig. 2*B*). Densitometry showed that we obtained essentially complete replacement of the endogenous protein with the transgenically-encoded cTnI$^{\Delta 2-11}$ in line 93, which was chosen for subsequent functional analyses. Replacement of endogenous cTnI with cTnI$^{\Delta 2-11}$ had no effect on expression levels of the other major contractile proteins, including MyHC, actin, myosin light chains, cTnT and α-TM (Fig. 2*A*). The deletion of the acidic-N′-region of cTnI was benign with no signs of increased morbidity, mortality or cardiac hypertrophy, implying that cTnI$^{\Delta 2-11}$ is functionally active. Heart weight/body weight (HW/BW) ratios did not differ significantly between NTG (0.0051 ± 0.006, n = 8) and cTnI$^{\Delta 2-11}$ (0.0050 ± 0.005, n = 6) littermates. The cTnI$^{\Delta 2-11}$ hearts were unremarkable and showed no evidence of abnormal morphology, myofibrillar disarray, necrosis, or ventricular fibrosis (Fig. 3*A* and *B*). Normal integration of cTnI$^{\Delta 2-11}$ into the

sarcomere was confirmed by immunofluorescent detection using cTnI-specific antibodies (Fig. 3*C*).

Functional analyses of cTnI$^{\Delta 2-11}$ hearts

Although the TG animals appeared overtly normal and showed no obvious pathology, we hypothesized that the cTnI$^{\Delta 2-11}$ hearts would have reduced basal cardiac function and this deficit would remain or 9 become more pronounced during β-AR stimulation. To test this, NTG and cTnI$^{\Delta 2-11}$ animals underwent two weeks of continuous β-agonist infusion with isoproterenol (ISO). We utilized four, 12-week old groups; NTG (sham), NTG (ISO), cTnI$^{\Delta 2-11}$ (sham) and cTnI$^{\Delta 2-11}$ (ISO). At the end of the two-week infusion, cardiac function was assessed by M-mode echocardiography. Both the NTG and cTnI$^{\Delta 2-11}$ sham animals showed normal fractional shortening and the other functional parameters did not differ between the two groups (Fig. 4*A* and *C*, Table 1). In contrast, both the NTG and cTnI$^{\Delta 2-11}$ ISO groups had significantly increased left ventricular inner diameters in diastole and systole and decreased fractional shortening. Importantly, significant differences presented between the NTG and cTnI$^{\Delta 2-11}$ groups, with the cTnI$^{\Delta 2-11}$ ISO hearts displaying both decreased heart rates and fractional shortening compared to the NTG ISO hearts. Continuous ISO infusion increased the HW/BW ratio significantly in both NTG and cTnI$^{\Delta 2-11}$ ISO groups compared to the respective sham groups but no differences presented between the NTG and cTnI$^{\Delta 2-11}$ ISO groups, ruling out a differential hypertrophic response as being responsible for the functional differences that were observed (Fig. 4*B* and *D*).

After the two-week infusion, *in vivo* hemodynamics were determined using the closed chest model and invasive catheterization (EXPERIMENTAL PROCEDURES). Ventricular contraction and relaxation were measured at baseline and during dobutamine infusion. As expected, dobutamine infusion increased dP/dt_{max} and dP/dt_{min} in both the NTG and cTnI$^{\Delta 2-11}$ sham hearts (Fig. 4*E* and *F*) but basal and stimulated values for both these parameters were decreased in the cTnI$^{\Delta 2-11}$ hearts as compared to the NTG hearts. That is, dP/dt_{max} increased in NTG sham hearts by 50% at the highest dobutamine dose, but only by 30% in the cTnI$^{\Delta 2-11}$ sham hearts (Fig. 4*E* and *F*, Table 2). After two weeks of continuous ISO infusion, the cTnI$^{\Delta 2-11}$ ISO hearts displayed a relatively depressed heart rate at baseline and upon dobutamine infusion (Table 2). Hemodynamic parameters, including LV pressure, dP/dt_{max} and dP/dt_{min} were also significantly compromised in the cTnI$^{\Delta 2-11}$ ISO hearts, compared to the NTG ISO group (Table 2). The NTG ISO hearts showed conserved cardiac function with values for both dP/dt_{max} and dP/dt_{min} at baseline almost equivalent to the rates that obtained with a maximum dose of dobutamine in the NTG sham mice. As expected, NTG ISO hearts were unable to respond to increasing concentrations of dobutamine as they were already fully stimulated. These results indicate that, despite appearing overtly normal and healthy under standard cage conditions, the acidic-N′-region deletion does compromise cardiac function and this is exacerbated under conditions of chronic and acute β-AR stimulation.

Actomyosin Ca^{2+}-activated maximal Mg^{2+}-ATPase and Ca^{2+} sensitivity

We used skinned papillary muscle fibers to assess the effect of cTnI$^{\Delta 2-11}$ on the kinetics and Ca^{2+} sensitivity of force generating cross-bridge formation. Fiber preparations were also subjected to PKA treatment in order to compare fully phosphorylated cTnI with the truncated TG protein (Fig. 5*A*). Average maximally developed isometric tension (F_{max}) was significantly decreased in cTnI $^{2-11}$–derived fibers relative to NTG fibers (8.9 ± 0.4 versus 6.9 ± 0.6 kN/m^2, $P<0.002$, n = 5), although Ca^{2+} sensitivity was unaffected. The same fibers were then treated with PKA and the effects on Ca^{2+} sensitivity and maximum force determined for both the NTG and cTnI$^{\Delta 2-11}$ fibers. Exogenous treatment of fibers with PKA did not affect F_{max} in either group (Table 3). Ca^{2+} sensitivity was significantly decreased by PKA treatment compared to the untreated fibers for both groups. In this isolated system, cTnI$^{\Delta 2-11}$'s effect on

maximal force development is consistent with decreased myocardial contractility *in vivo* and a concomitant decrease in the number of force-generating cross-bridges. There was no difference in the basal and PKA-activated Ca^{2+}-sensitivity, indicating that the deletion did not affect phosphorylation of $Ser^{23/24}$ or myofilament Ca^{2+} sensitivity.

To understand the consequences of $cTnI^{\Delta 2-11}$ on the Ca^{2+} activated actomyosin Mg^{2+}-ATPase activity, myofibril Mg^{2+}-ATPase activity and Ca^{2+} sensitivity were measured with or without PKA treatment (Fig. 5*B* and Table 4). The $cTnI^{\Delta 2-11}$ myofibrils showed a significant decrease in the maximal Mg^{2+}-ATPase activity (163.07 ± 4.85 nmol P_i/min/mg, $P<0.01$) compared to the NTG (188.96 ± 4.67 nmol P_i/min/mg) but Ca^{2+} sensitivity was unaffected. As expected, PKA treatment of either $cTnI^{\Delta 2-11}$ or NTG myofibrils resulted in decreased Ca^{2+} sensitivity. Hill coefficients and EC_{50} values fall within the range of those previously reported (8). The Hill coefficients for the NTG and $cTnI^{\Delta 2-11}$ proteins did not differ, reflecting the similarities in the shape of the Ca^{2+} binding curves. Phosphorylation of cTnI residues was confirmed by Western blots using phospho-specific cTnI antibodies (Fig. 5*B*, inset). Taken together, the data show that the acidic-N′-region plays a major role in regulating the actomyosin Ca^{2+}-activated maximal Mg^{2+}-ATPase activity.

To confirm that these functional, hemodynamic and biochemical changes were not due to compensatory changes in contractile protein phosphorylation states, PLN (Fig. 6*A*), the myosin light chains (Fig. 6*B*) and cMyBP-C (Fig. 6*C*) phosphorylation was examined by Western blot analysis using phospho-specific antibodies and two-dimensional electrophoresis. The data showed that phosphorylation levels of these proteins were unchanged between the $cTnI^{\Delta 2-11}$ and NTG sham and ISO hearts, respectively.

Structural and computational analysis of $cTnI^{\Delta 2-11}$

Backbone amide resonances provide excellent probes for monitoring protein-protein interactions and identifying interaction surfaces. The chemical shift differences can be used to map the cTnC binding site of the N′-extension (2–33) of cTnI on Ca^{2+}-loaded cTnC. Interactions of the N′-extension (2–33) and, in particular, the conserved acidic-N′-region (2–11) were analyzed by comparing combined amide ^1H and ^{15}N chemical shift differences for Ca^{2+}-loaded cTnC bound to cTnI and $cTnI^{\Delta 2-33}$ (Fig. 7*A*) and for cTnC bound to cTnI and $cTnI^{\Delta 2-11}$ (Fig. 7*B*). Residues showing significant chemical shift perturbations induced by the N′-extension (2–33) were located in the N′-lobe of cTnC with the largest perturbations centered in defunct Ca^{2+}-binding site I (28–38) and Ca^{2+} binding site II (65–76) (Fig. 1*A*). Bis-phosphorylation or introduction of negative charge at $Ser^{23/24}$ in the N′-extension results in a loss of these interactions (10,11,19). No significant chemical shift perturbations were observed in the linker region or in the C′-lobe of cTnC. Composite amide ^1H and ^{15}N chemical shift differences for Ca^{2+}-loaded cTnC bound to cTnI and $cTnI^{\Delta 2-11}$ were considerably smaller, generally <0.05 ppm (Fig. 7*B*). The magnitude of the observed chemical shift perturbations suggest that residues 2–11, comprising the conserved acidic N′-region, do not interact strongly with Ca^{2+}-loaded cTnC. This is consistent with previously published chemical shift perturbation analysis (19,20) and binding studies (21) supporting interactions between residues 19–30 in the N′-extension and the N′-lobe of Ca^{2+}-loaded cTnC.

Amide proton and amide nitrogen chemical shifts of residues in the N′-lobe of cTnC can be used to monitor opening of the regulatory domain upon binding cTnI (19,20). The conformational transitions for two residues, Glu^{66} and Ile^{128}, located in the N′- and C′-lobes of cTnC respectively, were examined in detail. Glu^{66} can exhibit conformational dependent chemical shift changes that are correlated with open and closed N′-lobe conformations (20). The binding of full-length cTnI to Ca^{2+}-loaded cTnC results in a downfield shift for the amide cross-peak of Glu^{66} (Fig. 7*C*). This shift is consistent with an opening of the N′-lobe of cTnC and exposure of the hydrophobic cleft for binding the switch region of cTnI (20). A similar

downfield shift for the amide cross-peak of Glu^{66} is observed in the presence of $cTnI^{\Delta 2-11}$ (Fig. 7*C*). However, the magnitude of the shift is intermediate between that observed for free Ca^{2+}-loaded cTnC and the Ca^{2+}-loaded cTnC/cTnI complex (Fig. 7*C*). The magnetically different amide ^{1}H-^{15}N environments presumably result from alterations in the N′-lobe open/closed equilibrium (20), indicating that the conserved acidic-N′-region (2–11) shows some propensity for stabilizing a more open N′-lobe conformation. Loss of the conserved acidic-N′-region may alter the interaction of residues 19–30 of cTnI with the N′-lobe of cTnC. It is known that phosphorylation of $Ser^{23/24}$ of cTnI results in weakening of the interactions between the N′-extension and the N′-lobe of cTnC, providing a molecular basis by which the N′-lobe conformational equilibrium is modified in response to physiological stimuli (20). No significant chemical shift changes in Ile^{128} were observed between Ca^{2+}-loaded cTnC and Ca^{2+}-loaded cTnC bound to either cTnI or $cTnI^{\Delta 2-11}$ (Fig. 7*C*).

DISCUSSION

Human cTnI has a 31-residue N′-extension that is not present in the fast and slow skeletal muscle isoforms. This extension contains a unique acidic-N′-region, a Xaa-Pro region (12–18) and a bisphosphorylation motif, in which $Ser^{23/24}$ are substrates for PKA, PKD and the Rho kinases. Bisphosphorylation at $Ser^{23/24}$ in the N′-extension of cTnI, in response to β-adrenergic stimulation, modulates myofilament Ca^{2}-sensitivity and cross-bridge kinetics (5, 7). The extension is highly conserved among mammals and its functional importance underscored by the finding of two missense mutations within the N′-extension that cause familial hypertrophic cardiomyopathy (FHC) in humans (15,16). One mutation, FHC^{A2V} (22), is located in the acidic-N′-region and the second, FHC^{R21C}, in the phosphorylation motif (23). Although NMR and modeling studies have shown that the conserved acidic-N′-region of the N′-extension can extend from its position on the N-lobe of cardiac troponin C (cTnC) and interact with the basic inhibitory region of cTnI, the role of the acidic N′-region of cTnI in the modulation of cardiac contractility is not clear. A novel finding reported in the present study is the reduction of rate of contractile function at baseline and β-AR stimulation in $cTnI^{\Delta 2-11}$ hearts lacking the acidic N-terminus region of cTnI. The TG mice expressing cardiac-specific $cTnI^{\Delta 2-11}$ were allowed to determine the role of acidic-N′-region of cTnI on myocardial function and response to β-AR stimulation. $cTnI^{\Delta 2-11}$ maintains the core structure of cTnI and thus wouldn't modify the troponin complex as reported in previous studies (24,25). $cTnI^{\Delta 2-11}$ hearts, with >95% of cTnI replaced by $cTnI^{\Delta 2-11}$, appeared apparently normal. The $cTnI^{\Delta 2-11}$ is benign without any obvious increased mortality or detectable cardiovascular pathology. The $cTnI^{\Delta 2-11}$ mice were viable and fertile and exhibited normal ventricular weights and heart rates; however, significant differences in contractile function were evident. This data suggests that removal of acidic-N′-region of cTnI wouldn't affect the heart adversely. Similar findings were observed in cardiac-specific TG mice that express either lack of the N′-extension 2–28 residues of cTnI (24) or replacement of cTnI with the slow skeletal TnI (25), that differ from cTnI by the absence of unique 32 residues at the N′-extension of cTnI. Conversely, the mice (18) and rabbits (26) expressing $cTnI^{146Gly}$, a FHC mutation that is located within the inhibitory region, resulted in cardiomyocytes disarray, interstitial fibrosis and suffered premature death.

In the present study, the absolute force and Mg^{2+}-ATPase activity data follow the same pattern in $cTnI^{\Delta 2-11}$ myofilaments. The expected decrease in maximal force and actomyosin Mg^{2+}-ATPase activity as a result of $cTnI^{\Delta 2-11}$ was confirmed in the skinned fiber studies with no change in Ca^{2+} sensitivity of the $cTnI^{\Delta 2-11}$. Our data further show that the $Ser^{23/24}$ phosphorylation and Ca^{2+} binding sites are unaltered by incorporation of $cTnI^{\Delta 2-11}$. Thus, we think that the deletion alters the orientation of the N′-extension of cTnI, which then affects the interaction between the acidic-N′-region and the inhibitory domain of cTnI with cTnC and actin. In addition, a basic C′-region of cTnI, not observed in the cTnI crystal structure (27) can

interact electrostatically with actin (28). Modeling studies suggest that Ca^{2+}-induced translocation of cTnI's mobile C- terminal domain to actin is triggered by the switch region's binding to the N′-lobe of cTnC. Thus, in the low $Ca^{2+\Delta}$state, both the inhibitory region and mobile C-terminal domain of cTnI bind to actin, forming an electrostatic clamp that pushes tropomyosin toward the outer domain of actin (28). Our studies indicate that the acidic-N′-region of cTnI plays an active role in modulating the interactions of the inhibitory region and the C-terminal mobile domain of cTnI with α-actin, which could influence the position of tropomyosin binding on actin. Protein-protein interactions within tropomyosin can influence the movement and position of tropomyosin on the actin surface (29).

$Ser^{23/24}$ phosphorylation within the N′-extension of cTnI results in a reduction in myofilament Ca^{2+} sensitivity, an increase in cross-bridge cycling, and enhanced binding of cTnI to the thin filament (7,8,30,31). Studies in the intact heart have demonstrated a significant role of cTnI phosphorylation for both afterload dependence of ejection and relaxation (32) as well as force frequency modulation (30). To determine the functional consequences of the acidic-N′-region upon *β*-AR stimulation, we examined contraction and relaxation under baseline conditions and during *β*-AR stimulation. Incorporation of $cTnI^{\Delta 2-11}$ into the sarcomere reduces baseline values for dP/dt_{max} and dP/dt_{min}, indicating a negative regulatory mechanism of cardiac function followed by decreased maximal force and Mg^{2+}-ATPase activity. Moreover, during chronic long-term *β*-AR stimulation with ISO, contractile function was blunted in the $cTnI^{\Delta 2-11}$ mouse hearts. We were able to exclude the possibility that alterations in either phosphorylation levels or expression levels of the cMyBP-C, myosin light chains and PLN were compensating for a reduction in contractile function in the $cTnI^{\Delta 2-11}$ hearts. Consistent with altered interactions of mutant cTnI with the cTnC and actin, TG mice that express a cTnI which lacks residues 2–28 (24) and the $cTnI^{146Gly}$ (18) showed enhanced contractility with impaired relaxation at the whole heart level.

NMR data and sequence analyses indicate a loosely structured N′-extension with a propensity for a helical region surrounding the bisphosphorylation motif (20–24), followed by a helical C-terminal region in residues 25–30 (Rosevear *et al.*, unpublished data). An extended poly(L-proline)II helix (11–19) appears to serve as a rigid linker that aids in positioning the acidic-N′-region. In this conformation, the N′-extension of cTnI interacts with the N′-lobe of troponin C (cTnC), modulating myofilament Ca^{2+}-sensitivity. Introduction of a negative charge at $Ser^{23/24}$ via phosphorylation weakens its interaction with the N′-lobe of cTnC by repositioning the extension. NMR studies (9,11,19,20,33), binding studies (34), deletion mutagenesis (21), and cross-linking studies (35) have shown that the N′-extension of cTnI interacts with the N′-lobe of cTnC. Specifically, these studies defined residues 19–30 as the minimal region of the N′-extension necessary for interacting with the N′-lobe of cTnC. Residues surrounding the inactive Ca^{2+} binding site I in cTnC may comprise the potential interaction site with the N′-extension. NMR studies further showed that interaction of the cardiac N-extension alters N′-lobe conformational equilibria in cTnC toward a more active/open conformation capable of binding the switch region of cTnI (9,20,34). Bisphosphorylation at $Ser^{23/24}$ in the N′-extension results in the loss of N′-lobe interactions, shifting the N′-lobe conformational equilibrium toward a more closed conformation, resulting in decreased Ca^{2+} sensitivity. This mechanism utilizes the unique isoform differences in both cTnC and cTnI, providing a molecular switch for modulating cardiac muscle contraction.

The roles of the conserved Xaa-Pro and acidic-N′-region in the N′-extension remain relatively undefined. Recent structural studies from one of our laboratories (P.R.) on the phosphorylation of $Ser^{23/24}$ showed that the Xaa-Pro region forms an extended polyproline helix (unpublished data), possibly providing a rigid spacer for interaction of the acidic-N′-region with basic regions within the troponin complex, inducing a bending in the rod-like cTnI at the end that interacts with the cTnC/cTnT component (36). Furthermore, we constructed atomic models for troponin

that show the conformational transition induced by bisphosphorylation, based on the structure of the bisphosphorylated N′-extension, the X-ray crystal structure of the cardiac troponin core (27), and the uniform density models of the troponin components derived from neutron contrast variation data (36). Therefore, we hypothesize that the acidic-N′-region interacts with the basic residues in its inhibitory region, competing with actin for the inhibitory region of cTnI or the second actin-binding region of cTnI (Fig. 8) and is responsible for altering cross-bridge kinetics.

Our data are consistent with the hypothesis that removal of the acidic-N′-region from cTnI prevents interaction of this region with the inhibitory domain of cTnI, permitting it to associate more readily with actin. As a result, enhancing the contact between actin and the inhibitory domain of cTnI might ultimately diminish cardiac contractility and maximal force of contraction. In support of our proposed model, the $cTnI^{\Delta 2-11}$ myofilaments showed decreased maximal absolute force and Mg^{2+}-ATPase activity, leading to reduction of contractile function at baseline and during β-AR stimulation. Taken together, the data indicate that the interaction of the acidic-N′-region with the inhibitory region of cTnI provides a novel mechanism by which the acidic-N′-region modulates cross-bridge kinetics and regulates actomyosin interactions. Additional biochemical and structural studies are warranted to gain insight into the molecular function of the acidic-N′-region and its roles in cardiac muscle acidosis and regulation of contraction.

Acknowledgements

This research was supported by National Institutes of Health grants HL69799, HL60546, HL52318, HL60546, and HL56370 (J.R.) and by the American Heart Association, Ohio Valley Affiliate (S.S.) and United States Department of Defense Grant ARO MURI DAAD 19-02-1-0027 (PRR).

References

1. Kranias EG, Solaro RJ. Phosphorylation of troponin I and phospholamban during catecholamine stimulation of rabbit heart. Nature 1982;298:182–184. [PubMed: 6211626]
2. Murphy AM, Jones L 2nd, Sims HF, Strauss AW. Molecular cloning of rat cardiac troponin I and analysis of troponin I isoform expression in developing rat heart. Biochemistry 1991;30:707–712. [PubMed: 1988058]
3. Sasse S, Brand NJ, Kyprianou P, Dhoot GK, Wade R, Arai M, Periasamy M, Yacoub MH, Barton PJ. Troponin I gene expression during human cardiac development and in end-stage heart failure. Circ Res 1993;72:932–938. [PubMed: 8477526]
4. Saggin L, Gorza L, Ausoni S, Schiaffino S. Troponin I switching in the developing heart. J Biol Chem 1989;264:16299–16302. [PubMed: 2777792]
5. Chandra M, Dong WJ, Pan BS, Cheung HC, Solaro RJ. Effects of protein kinase A phosphorylation on signaling between cardiac troponin I and the N-terminal domain of cardiac troponin C. Biochemistry 1997;36:13305–13311. [PubMed: 9341222]
6. Haworth RS, Cuello F, Herron TJ, Franzen G, Kentish JC, Gautel M, Avkiran M. Protein kinase D is a novel mediator of cardiac troponin I phosphorylation and regulates myofilament function. Circ Res 2004;95:1091–1099. [PubMed: 15514163]
7. Kentish JC, McCloskey DT, Layland J, Palmer S, Leiden JM, Martin AF, Solaro RJ. Phosphorylation of troponin I by protein kinase A accelerates relaxation and crossbridge cycle kinetics in mouse ventricular muscle. Circ Res 2001;88:1059–1065. [PubMed: 11375276]
8. Sakthivel S, Finley NL, Rosevear PR, Lorenz JN, Gulick J, Kim S, VanBuren P, Martin LA, Robbins J. In vivo and in vitro analysis of cardiac troponin I phosphorylation. J Biol Chem 2005;280:703–714. [PubMed: 15507454]
9. Abbott MB, Dong WJ, Dvoretsky A, DaGue B, Caprioli RM, Cheung HC, Rosevear PR. Modulation of cardiac troponin C-cardiac troponin I regulatory interactions by the amino-terminus of cardiac troponin I. Biochemistry 2001;40:5992–6001. [PubMed: 11352734]

10. Abbott MB, Dvoretsky A, Gaponenko V, Rosevear PR. Cardiac troponin I inhibitory peptide: location of interaction sites on troponin C. FEBS Lett 2000;469:168–172. [PubMed: 10713265]
11. Finley N, Abbott MB, Abusamhadneh E, Gaponenko V, Dong W, Gasmi-Seabrook G, Howarth JW, Rance M, Solaro RJ, Cheung HC, Rosevear PR. NMR analysis of cardiac troponin C-troponin I complexes: effects of phosphorylation. FEBS Lett 1999;453:107–112. [PubMed: 10403385]
12. Sadayappan S, Gulick J, Osinska H, Martin LA, Hahn HS, Dorn GW 2nd, Klevitsky R, Seidman CE, Seidman JG, Robbins J. Cardiac myosin-binding protein-C phosphorylation and cardiac function. Circ Res 2005;97:1156–1163. [PubMed: 16224063]
13. El-Armouche A, Boknik P, Eschenhagen T, Carrier L, Knaut M, Ravens U, Dobrev D. Molecular determinants of altered Ca2+ handling in human chronic atrial fibrillation. Circulation 2006;114:670–680. [PubMed: 16894034]
14. D'Angelo DD, Sakata Y, Lorenz JN, Boivin GP, Walsh RA, Liggett SB, Dorn GW 2nd. Transgenic Galphaq overexpression induces cardiac contractile failure in mice. Proc Natl Acad Sci U S A 1997;94:8121–8126. [PubMed: 9223325]
15. Krenz M, Robbins J. Impact of beta-myosin heavy chain expression on cardiac function during stress. J Am Coll Cardiol 2004;44:2390–2397. [PubMed: 15607403]
16. Fewell JG, Hewett TE, Sanbe A, Klevitsky R, Hayes E, Warshaw D, Maughan D, Robbins J. Functional significance of cardiac myosin essential light chain isoform switching in transgenic mice. J Clin Invest 1998;101:2630–2639. [PubMed: 9637696]
17. Krenz M, Sadayappan S, Osinska HE, Henry JA, Beck S, Warshaw DM, Robbins J. Distribution and structure-function relationship of myosin heavy chain isoforms in the adult mouse heart. J Biol Chem. 2007in press
18. James J, Zhang Y, Osinska H, Sanbe A, Klevitsky R, Hewett TE, Robbins J. Transgenic modeling of a cardiac troponin I mutation linked to familial hypertrophic cardiomyopathy. Circ Res 2000;87:805–811. [PubMed: 11055985]
19. Gaponenko V, Abusamhadneh E, Abbott MB, Finley N, Gasmi-Seabrook G, Solaro RJ, Rance M, Rosevear PR. Effects of troponin I phosphorylation on conformational exchange in the regulatory domain of cardiac troponin C. J Biol Chem 1999;274:16681–16684. [PubMed: 10358006]
20. Abbott MB, Gaponenko V, Abusamhadneh E, Finley N, Li G, Dvoretsky A, Rance M, Solaro RJ, Rosevear PR. Regulatory domain conformational exchange and linker region flexibility in cardiac troponin C bound to cardiac troponin I. J Biol Chem 2000;275:20610–20617. [PubMed: 10801883]
21. Ward DG, Cornes MP, Trayer IP. Structural consequences of cardiac troponin I phosphorylation. J Biol Chem 2002;277:41795–41801. [PubMed: 12207022]
22. Murphy RT, Mogensen J, Shaw A, Kubo T, Hughes S, McKenna WJ. Novel mutation in cardiac troponin I in recessive idiopathic dilated cardiomyopathy. Lancet 2004;363:371–372. [PubMed: 15070570]
23. Arad M, Penas-Lado M, Monserrat L, Maron BJ, Sherrid M, Ho CY, Barr S, Karim A, Olson TM, Kamisago M, Seidman JG, Seidman CE. Gene mutations in apical hypertrophic cardiomyopathy. Circulation 2005;112:2805–2811. [PubMed: 16267253]
24. Barbato JC, Huang QQ, Hossain MM, Bond M, Jin JP. Proteolytic N-terminal truncation of cardiac troponin I enhances ventricular diastolic function. J Biol Chem 2005;280:6602–6609. [PubMed: 15611140]
25. Fentzke RC, Buck SH, Patel JR, Lin H, Wolska BM, Stojanovic MO, Martin AF, Solaro RJ, Moss RL, Leiden JM. Impaired cardiomyocyte relaxation and diastolic function in transgenic mice expressing slow skeletal troponin I in the heart. J Physiol 1999;517(Pt 1):143–157. [PubMed: 10226156]
26. Sanbe A, James J, Tuzcu V, Nas S, Martin L, Gulick J, Osinska H, Sakthivel S, Klevitsky R, Ginsburg KS, Bers DM, Zinman B, Lakatta EG, Robbins J. Transgenic rabbit model for human troponin I-based hypertrophic cardiomyopathy. Circulation 2005;111:2330–2338. [PubMed: 15867176]
27. Takeda S, Yamashita A, Maeda K, Maeda Y. Structure of the core domain of human cardiac troponin in the Ca(2+)-saturated form. Nature 2003;424:35–41. [PubMed: 12840750]
28. Murakami K, Yumoto F, Ohki SY, Yasunaga T, Tanokura M, Wakabayashi T. Structural basis for Ca2+-regulated muscle relaxation at interaction sites of troponin with actin and tropomyosin. J Mol Biol 2005;352:178–201. [PubMed: 16061251]

29. Holthauzen LM, Correa F, Farah CS. Ca2+-induced rolling of tropomyosin in muscle thin filaments: the alpha- and beta-band hypothesis revisited. J Biol Chem 2004;279:15204–15213. [PubMed: 14724287]

30. Takimoto E, Soergel DG, Janssen PM, Stull LB, Kass DA, Murphy AM. Frequency- and afterload-dependent cardiac modulation in vivo by troponin I with constitutively active protein kinase A phosphorylation sites. Circ Res 2004;94:496–504. [PubMed: 14726477]

31. Turnbull L, Hoh JF, Ludowyke RI, Rossmanith GH. Troponin I phosphorylation enhances crossbridge kinetics during beta-adrenergic stimulation in rat cardiac tissue. J Physiol 2002;542:911–920. [PubMed: 12154188]

32. Layland J, Grieve DJ, Cave AC, Sparks E, Solaro RJ, Shah AM. Essential role of troponin I in the positive inotropic response to isoprenaline in mouse hearts contracting auxotonically. J Physiol 2004;556:835–847. [PubMed: 14966306]

33. Ward DG, Brewer SM, Gallon CE, Gao Y, Levine BA, Trayer IP. NMR and mutagenesis studies on the phosphorylation region of human cardiac troponin I. Biochemistry 2004;43:5772–5781. [PubMed: 15134451]

34. Ward DG, Brewer SM, Calvert MJ, Gallon CE, Gao Y, Trayer IP. Characterization of the interaction between the N-terminal extension of human cardiac troponin I and troponin C. Biochemistry 2004;43:4020–4027. [PubMed: 15049709]

35. Ward DG, Brewer SM, Cornes MP, Trayer IP. A cross-linking study of the N-terminal extension of human cardiac troponin I. Biochemistry 2003;42:10324–10332. [PubMed: 12939162]

36. Heller WT, Abusamhadneh E, Finley N, Rosevear PR, Trewhella J. The solution structure of a cardiac troponin C-troponin I-troponin T complex shows a somewhat compact troponin C interacting with an extended troponin I-troponin T component. Biochemistry 2002;41:15654–15663. [PubMed: 12501194]

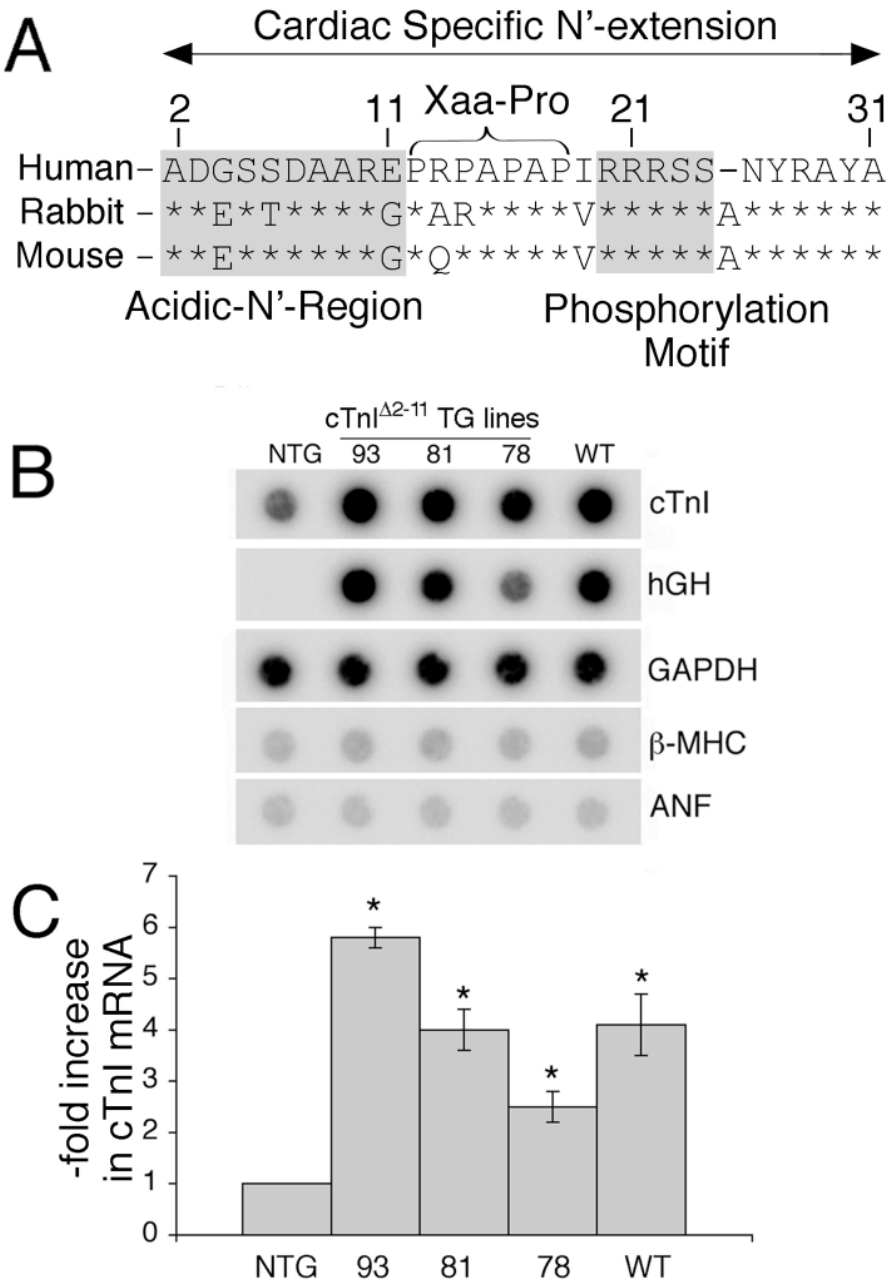

Figure 1.

Cardiac specific N′-extension and RNA expression in cTnI$^{\Delta 2–11}$ mice. *A*, Conserved N′-extension in cTnI. Amino acid residues identical to the human cTnI are represented by asterisks. The N′-extension, residues 1–31, is marked with arrows. The acidic-N′-region, which was deleted in the cTnI$^{\Delta 2–11}$ hearts, and the phosphorylation motif are each shaded and the polyproline (Xaa-Pro) spacer arm is indicated. *B*, RNA dot-blot analyses of cardiac gene expression in 12-week old cTnI$^{\Delta 2–11}$ TG lines (93, 81 and 78) compared to a NTG and cTnI^{WT} TG line (line 52 (18)). *C*, Fold changes in the amount of cTnI transcript levels normalized to GAPDH. Values are mean ± S.E. (n = 4). **P*<0.001.

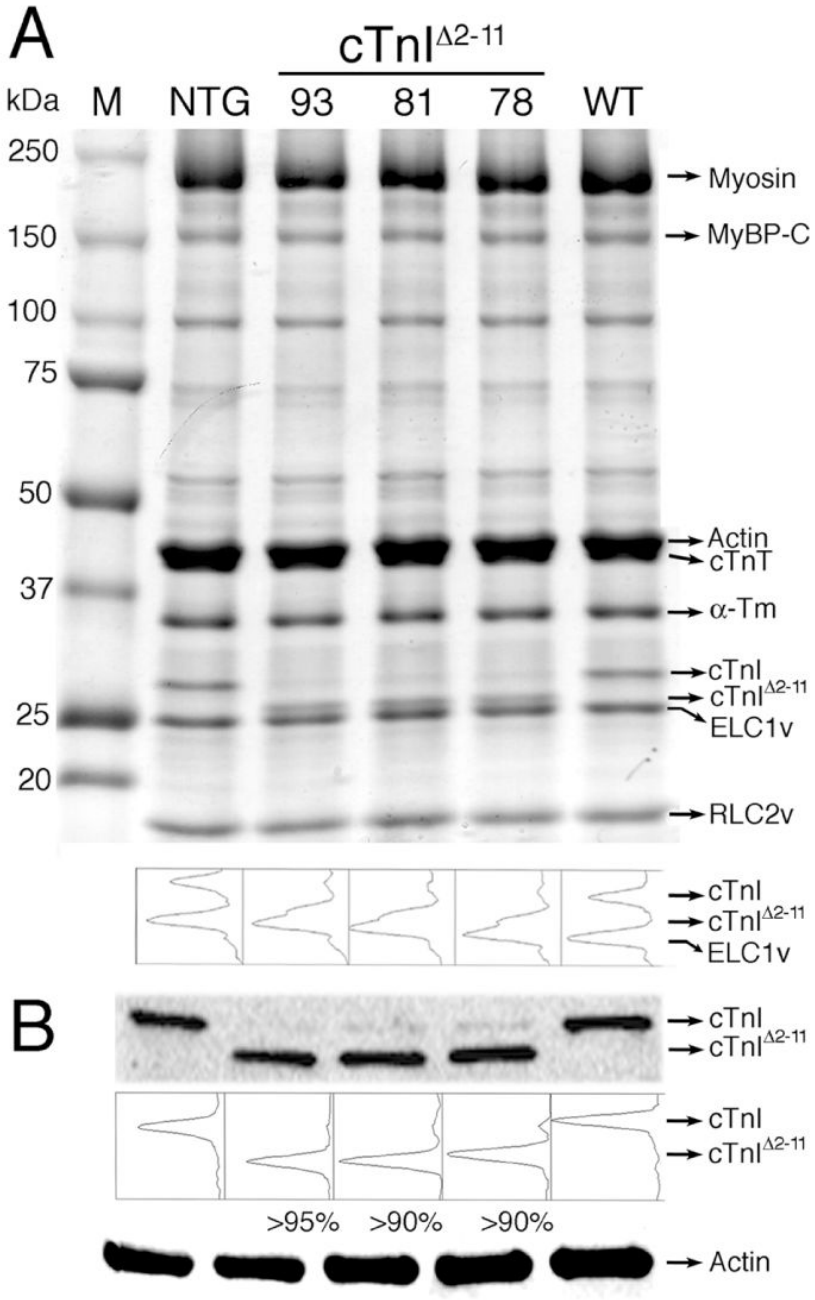

Figure 2.

Myofilament protein composition, expression of, and replacement with cTnI$^{\Delta 2-11}$. *A*, Total myofibrillar proteins from three TG lines generated with the cTnI$^{\Delta 2-11}$ construct were analyzed to determine the degree of cTnI$^{\Delta 2-11}$ replacement and conservation of the other sarcomeric protein levels. cTnI$^{\Delta 2-11}$ migrates faster in SDS-PAGE relative to endogenous cTnI due to the deletion of the first ten amino acids. The level of replacement can be clearly seen. A region of the gel containing cTnI, cTnI$^{\Delta 2-11}$ and ELC1v was scanned and the relative intensities are shown. *B*, Western analyses shows that cTnI$^{\Delta 2-11}$ expression did not alter the total cTnI protein content. A representative histogram of cTnI and cTnI$^{\Delta 2-11}$ is shown (n = 3). α-sarcomeric actin was used as a loading control.

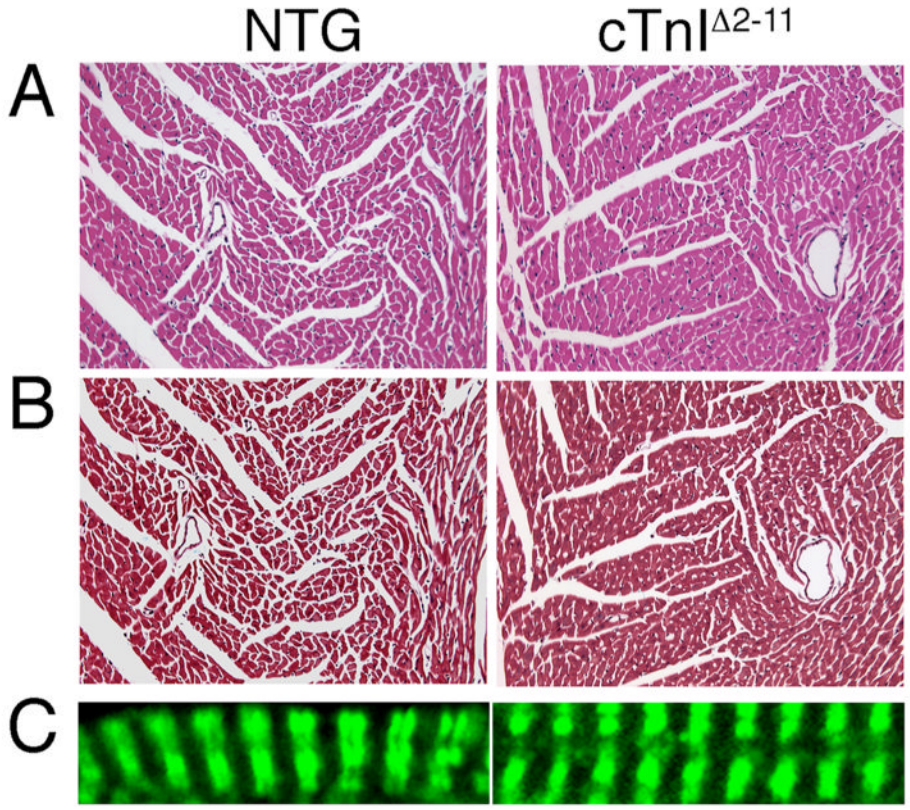

Figure 3.
Histopathological analyses. *A*, Longitudinal sections derived from 3 month old left ventricle stained with hematoxylin-eosin (*A*) or Masson trichrome (*B*) demonstrate the lack of obvious pathology (×20). *C*, Immunofluorescent staining of cTnI with anti-cTnI polyclonal antibodies shows normal incorporation into the sarcomere (×60).

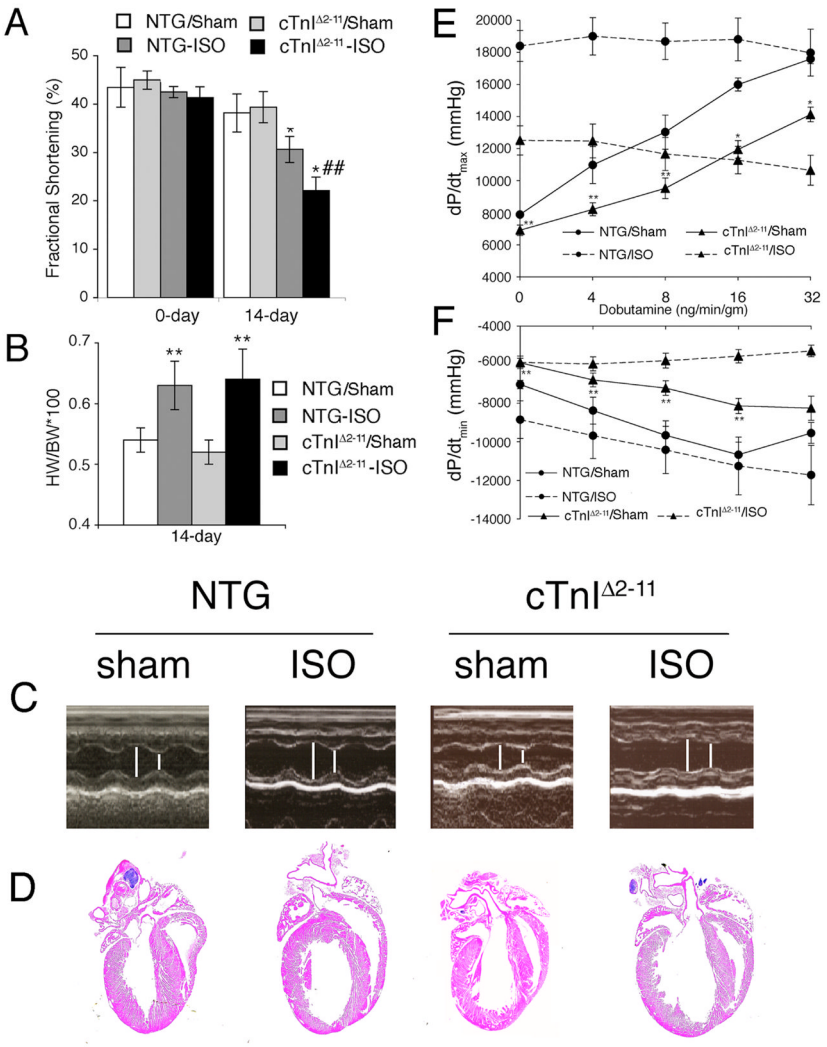

Figure 4.

In vivo cardiac function. Alzet osmotic minipumps (model 2002; Alza) that contained either ISO (60 mg/kg/day) or PBS (sham) were implanted dorsally and subcutaneously under isoflurane anesthesia. *In vivo* cardiac function was evaluated in the following groups; NTG/sham, NTG/ISO, cTnI$^{\Delta 2-11}$/sham and cTnI$^{\Delta 2-11}$/ISO. Mice were 12-weeks of age and were implanted with the pumps for a total of 14 days of stimulation. *A*, The fractional shortening (%) was measured by M-mode echocardiography. *Significant difference *versus* NTG (P<0.01, n = 6). ## Significant difference *versus* NTG-ISO (P<0.01, n = 6). *B*, HW/BW for adult mice. **Significant difference *versus* NTG (P<0.01, n = 6). *C*, M-mode echocardiographic tracings show LV dilation in the NTG/ISO and cTnI$^{\Delta 2-11}$/ISO hearts. *D*, Longitudinal sections stained with hematoxylin/eosin (x4) show enlarged LV in the NTG/ISO and cTnI$^{\Delta 2-11}$/ISO hearts. *E*, Maximal rate of ventricular contraction (dP/dt$_{max}$). *F*, Maximal rate of ventricular relaxation (dP/dt$_{min}$). Data were analyzed using a mixed, two-factor analysis of variance with repeated measures on the second factor. **P<0.01 and *P<0.001 significant difference *versus* NTG (n = 6). All data are presented as mean ± S.E.

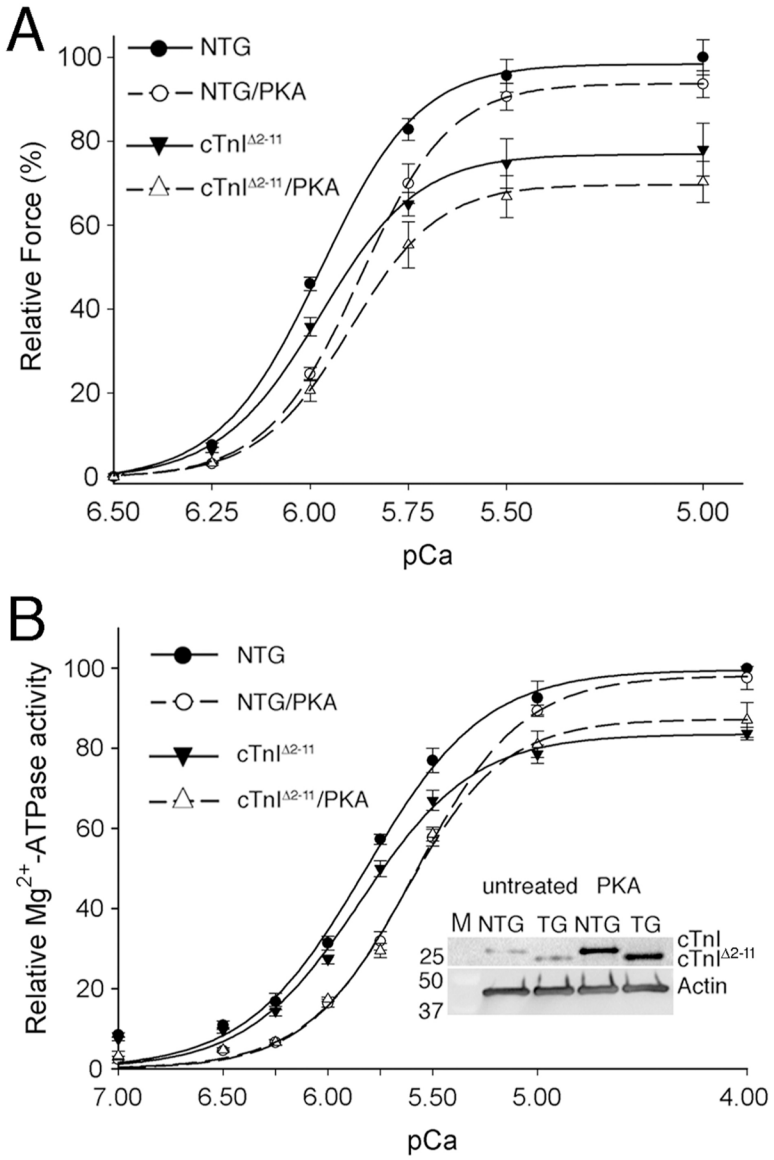

Figure 5.

In vitro skinned fiber analyses. *A*, Force-*p*Ca relationship of chemically skinned ventricular fibers before and after PKA-mediated phosphorylation. A bundle of 3–5 fibers isolated from glycerinated mouse papillary muscle fibers was attached by tweezer clips to a force transducer. After the initial steady state force was measured in *p*Ca 5.0 solution, the fiber bundles were exposed to increasing Ca^{2+} concentrations (from *p*Ca 8.0 to 5.0). After a contraction-relaxation cycle in the absence of PKA, the fibers were incubated with 0.5 μM PKA for 15 min at room temperature in relaxation solution (*p*Ca 8.0). A second contraction-relaxation cycle was subsequently obtained under the same conditions. Force is expressed as % of the force obtained at maximal Ca^{2+}-activation (*p*Ca 5.0). Values are mean ± S.E. (n = 5 per group, Table 3). *B*, Maximum Ca^{2+}-dependent Mg^{2+}-ATPase activity was determined at *p*Ca 4.0. Activity measured at *p*Ca 8.0 was subtracted and the activity at each *p*Ca value normalized to the maximum at *p*Ca 4.0 for each experiment. Data points represent the mean ± S.E. of five separate experiments in triplicate (Table 4). $cTnI^{\Delta 2–11}$ myofibrils showed significantly reduced maximal Mg^{2+}-ATPase activity under baseline and PKA treatment compared to NTG. In

contrast, there were no differences in the Ca^{2+} sensitivity between NTG and $cTnI^{\Delta 2–11}$ myofibrils. *Inset*: A representative immunoblot shows cTnI phosphorylation at $Ser^{23/24}$ by PKA (*upper panel*). The blot shows protein derived from NTG and $cTnI^{\Delta 2–11}$ (TG) hearts, untreated or treated with PKA, with phospho-cTnI antibody used as probe. *Lower panel*, α-sarcomeric actin staining confirms equal loading.

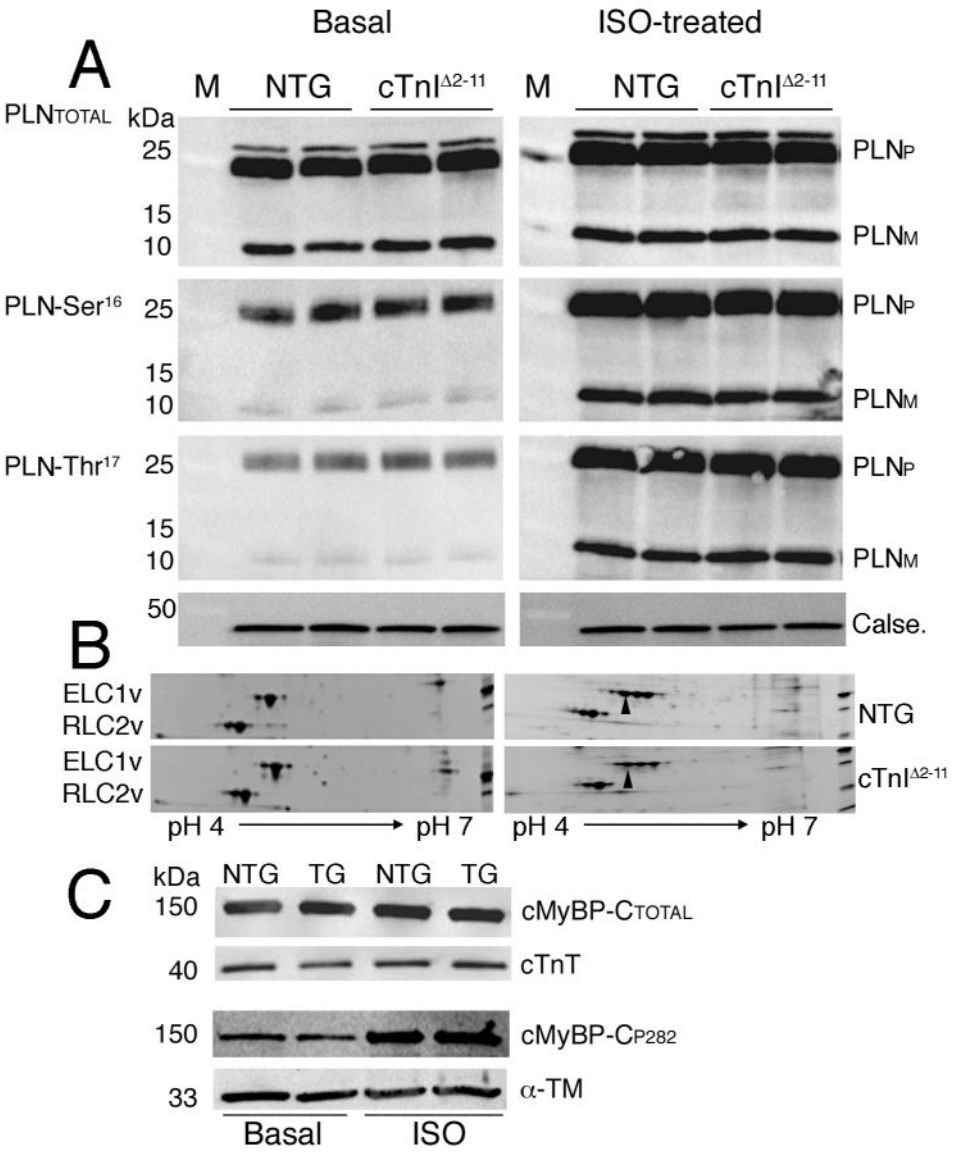

Figure 6.

Phosphorylation of PLN and myosin light chains. Cardiac total homogenates (10 μg) were subjected to 4–15% SDS-PAGE, electroblotted onto nitrocellulose membranes and probed with the indicated antibodies. *A*, Analyses of total PLN (PLN-Total), phospho-Ser^{16} (PLN-Ser^{16}) and phospho-Thr^{17} (PLN-Thr^{17}). PLN$_M$ and PLN$_P$ indicate monomeric and pentameric forms of PLN, respectively. Calsequestrin (Calse.) was used as a loading control. *B*, Representative SYPRO Ruby® stained 2D SDS- PAGE showing the phosphorylated species (arrowheads) of the essential light chain 1v (ELC1v) and regulatory light chain 2v (RLC2v). Total myofibrillar protein (75 μg) from ventricles were separated in the pH range of 4–7. *C*, cMyBP-C phosphorylation states in the NTG and TG groups were compared by Western blot analysis with 5 μg of protein isolated from 12 week old mouse hearts. Antibodies against cMyBP-C and phospho-cMyBP-C (pSer282) were used. Protein loading was normalized using total cardiac troponin T (cTnT) and cardiac α-tropomyosin (α-TM) antibodies. PLN, myosin

light chains and cMyBP-C phosphorylation levels did not differ between the NTG and cTnI$^{\Delta 2-11}$ (TG) groups at baseline, or between the groups after ISO treatment.

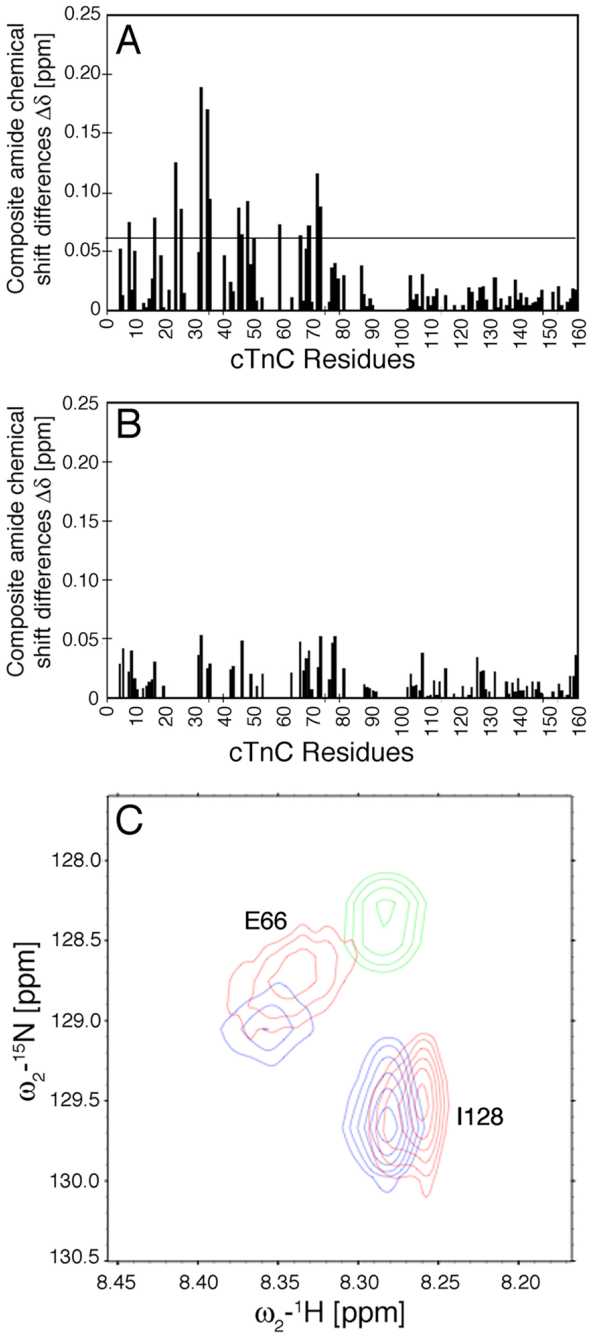

Figure 7.

Effect of cTnI$^{\Delta 2-11}$ on conformational exchange in the regulatory domain of cTnC. Combined amide proton and amide nitrogen absolute value chemical shift differences between (*A*) Ca^{2+}-loaded [^{15}N, ^{2}H]cTnC bound to cTnI$^{\Delta 2-33}$ and to cTnI$^{1-211}$ and (*B*) Ca^{2+}-loaded [^{15}N, ^{2}H] cTnC bound to cTnI$^{\Delta 2-11}$ and to cTnI$^{1-211}$. The horizontal bar represents the average chemical shift difference plus one standard deviation. The amide proton and amide nitrogen chemical shifts of resonances in the N′-lobe of cTnC can be used to monitor the opening of the regulatory domain upon binding cTnI. *C*, Overlapping segments of ^{15}N-^{1}H correlation spectra for residue E66 demonstrate the structural transition from the predominately “closed” N-domain of cTnC for the Ca^{2+}-loaded [^{15}N, ^{2}H]cTnC free in solution (green), to the partially “open” N′-lobe

conformation of Ca^{2+}-loaded [^{15}N, ^{2}H]cTnC bound to $cTnI^{\Delta 2–11}$ (red), and to the primarily "open" regulatory domain of Ca^{2+}-loaded [^{15}N, ^{2}H]cTnC bound to $cTnI^{1–211}$ (blue).

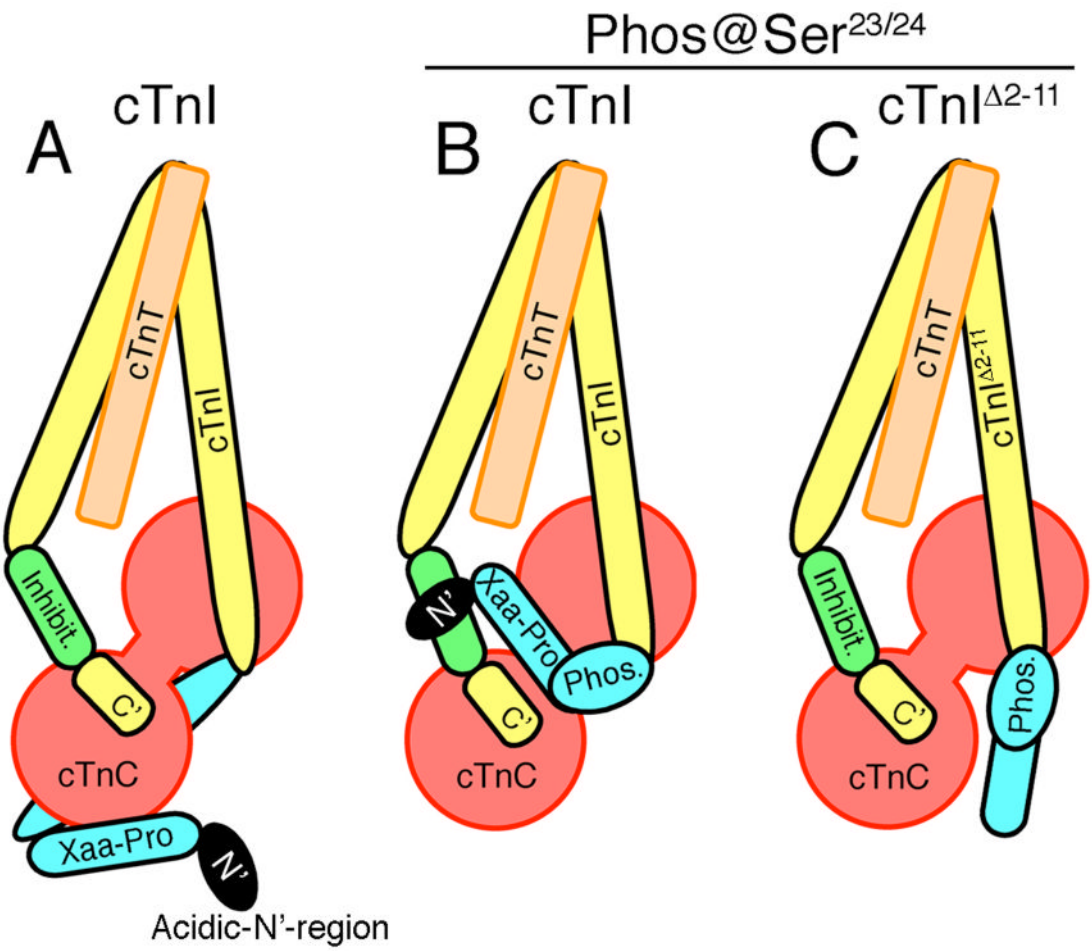

Figure 8.

Model of cTnI and effects of the cTnI$^{\Delta 2–11}$ deletion. Helices of cTnI and cTnT found in the core crystal structure of cardiac troponin are shown in yellow and orange, respectively (27). The inhibitory region of cTnI is shown in green. The Xaa-Pro regions of the N′-extension, residues 12–32 (Xaa-Pro) and the phosphorylation motif including Ser 23/24 (Phos.) are shown in blue. The acidic-N′-region (N′) of the N′-extension is shown in black. Cardiac TnC is shown in red. *A*, In the non-phosphorylated complex, the N′-extension of cTnI contacts the N′-lobe of cTnC. *B*, Bisphosphorylation at Ser$^{23/24}$ in the N′-extension induces a bending in the cTnI subunit, positioning the acidic-N′-region for electrostatic interactions with the inhibitory region of cTnI. *C*, Deletion of acidic-N′-region (residues 2–11) in bisphsosphorylated cTnI results in the loss of interaction between the N′-extension and the N′-lobe of cTnC, as well as the loss of electrostatic interactions between the acidic-N′-region and the inhibitory region of cTnI.

TABLE 1

Cardiac function assessed by M-mode echocardiography

	NTG	cTnI$^{\Delta 2–11}$	NTG/ISO	CTnI$^{\Delta 2–11}$/ISO
HR	465 ± 20	442 ± 25	609 ± 15^{a}	546 15,^{bc}
LVIDD	3.7 ± 0.07	3.6 ± 0.1	4.1 ± 0.1^{a}	4.2 ± 0.17^{b}
LVIDS	2.3 ± 0.06	2.2 ± 0.1	2.8 ± 0.07^{a}	3.2 ± 0.15,^{bc}
IVSTD	0.76 ± 0.03	0.7 ± 0.03	0.72 ± 0.01	0.73 ± 0.02
IVSTS	1.05 ± 0.05	1.0 ± 0.03	1.03 ± 0.02	0.93 ± 0.04
LVPWD	0.74 ± 0.03	0.7 ± 0.03	0.77 ± 0.02	0.71 ± 0.05
LVPWS	1.08 ± 0.03	1.02 ± 0.01	1.01 ± 0.02	0.97 ± 0.06
FS %	38 ± 0.8	39 ± 1.0	30 ± 1^{a}	23 ± 1,^{bc}

Measurement values in mm were averaged from at least 3 separate cardiac cycles: HR, heart rate (beats/min); LVIDD and LVIDS, left ventricular inner diameter in diastole and systole; IVSTD and IVSTS, inter-ventricular septum thickness in diastole and systole; LVPWD and LVPWS, left ventricular posterior wall thickness in diastole and systole; FS, left ventricular shortening fractional (%). The cTnI$^{\Delta 2–11}$ hearts demonstrated normal cardiac function compared to NTG cohorts. In contrast, the cTnI$^{\Delta 2–11}$/ISO hearts showed reduced cardiac function compared to NTG/ISO. Data are expressed as mean ± S.E. (n = 6).

^{a} $P<0.05$ significantly different from NTG sham,

^{b} $P<0.05$ significantly different from cTnI$^{\Delta 2–11}$ sham,

^{c} $P<0.05$ significantly different from NTG/ISO

TABLE 2

In vivo hemodynamic measurements

		At basal level		At saturated dobutamine dose (32ng/g/min)	
		NTG	**CTnI$^{\Delta 2-11}$**	**NTG**	**cTnI$^{\Delta 2-11}$**
Heart Rate (bpm)	Sham ISO	400 ± 28 625 ± 21^{a}	405 ± 15 538 ± 18^{b}	656 ± 46 620 ± 21	628 ± 28 373 ± 65^{b}
LVP (mm Hg/s)	Sham ISO	108 ± 17 93 ± 3	86 ± 6 80 ± 4	124 ± 19 101 ± 5	100 ± 6 73 ± 3^{b}
dP/dt_{max} (mm Hg/s)	Sham ISO	7895 ± 116 17594 ± 306^{a}	6906 ± 329^{a} 14131 ± 456^{b}	18401 ± 967 17980 ± 1458	12510 ± 906^{a} 10653 ± 937^{b}
dP/dt_{min} (mm Hg/s)	Sham ISO	−7029 ± 214 −8855 ± 979	−5906 ± 238^{a} −5876 ± 326^{b}	−9542 ± 537 −11725 ± 1534	−8256 ± 626^{a} −5287 ± 302^{b}

To evaluate LV function, telemetric measurements of heart rate (beats per minute (bpm)), left ventricular pressure (LVP) average maximum, the maximum rate of heart contraction (dP/dt_{max}) and relaxation (dP/dt_{min}) were measured in cTnI$^{\Delta 2-11}$ and NTG mice (12-week old). All data are presented as mean ± S.E (n = 6).

^{a}P<0.05 significantly different from sham NTG,

^{b}P<0.05 significantly different from ISO NTG)

TABLE 3

Ca^{2+}-activated maximum developed force

Genotype	PKA	F_{max}	EC_{50} for Ca^{2+}	Hill coefficient
NTG	Before	9.21 ± 0.28	5.78 ± 0.01	1.56 ± 0.07
	After	8.90 ± 0.37	5.64 ± 0.01[a]	1.45 ± 0.14
$CTnI^{\Delta 2-11}$	Before	6.52 ± 0.25[a]	5.79 ± 0.02	1.41 ± 0.09
	After	5.99 ± 0.10,[abc]	5.67 ± 0.01,[ac]	1.59 ± 0.11

All data are presented as mean ± S.E (n = 5). Maximum force (F_{max}) was measured at pCa 5.0.

[a] $P<0.05$ (compared to untreated NTG),

[b] $P<0.05$ (compared to PKA treated NTG),

[c] $P<0.05$ (compared to untreated $cTnI^{\Delta 2-11}$))

TABLE 4

Ca^{2+}-activated Mg^{2+}-ATPase activity

Genotype	PKA	V_{max}	EC_{50} for Ca^{2+}	Hill coefficient
NTG	Untreated	188.9 ± 4.7	5.78 ± 0.01	1.71 ± 0.06
	Treated	186.3 ± 5.3	5.56 ± 0.01[a]	1.82 ± 0.15
$CTnI^{\Delta 2-11}$	Untreated	163.1 ± 4.9[a]	5.76 ± 0.01	1.75 ± 0.05
	Treated	166.9 ± 8.2,[abc]	5.55 ± 0.03,[ac]	2.08 ± 0.27

All data are presented as mean ± S.E (n = 5). Maximum activity (V_{max}) was measured at pCa 4.0.

[a] $P<0.05$ (compared to untreated NTG),

[b] $P<0.05$ (compared to PKA treated NTG),

[c] $P<0.05$ (compared to untreated $cTnI^{\Delta 2-11}$))